

Electron irradiation effects on oxidized Nb foil and NbO

T. T. LIN*, DAVID LICHTMAN

Laboratory for Surface Studies and Department of Physics, University of Wisconsin-Milwaukee, Milwaukee, Wisconsin 53201, USA

Auger electron spectroscopy was used to study electron irradiation damage on niobium oxide. With the co-existence of O-2p and Nb-4d states in the valence band, the splitting of the MNN-type Auger transition peaks has been observed on Nb₂O₅ and oxidized Nb foil specimens. The results show that the surface of an electron-bombarded specimen becomes enriched with niobium due to irradiation-induced dissociation of the oxide and subsequent loss of oxygen. Supporting results obtained from electron stimulated desorption measurements, specimen coloration changes and layer-by-layer calculation of Auger intensity from an altered overlayer are also presented.

1. Introduction

The study of a solid surface subjected to photon-, neutron-, ion- or electron-bombardment can be divided into two parts: (1) investigation of the various properties of a beam-irradiated substrate. It has been found in many cases that certain substrate properties such as structure, conductivity, etc. are sensitive to beam exposure under particular conditions. (2) Studying the gases, ions and/or electrons released from the specimen surface. Valuable information, such as the identity of adsorbed species, the chemical bonding state of adsorbed species on the substrate, etc. can be deduced. This topic is not only interesting theoretically but also has important practical applications, for example, in catalysis and the so-called first-wall problem in controlled thermonuclear reactors (CTR). In the latter case, the reactor wall will be subjected to a wide range of beam irradiations. Two of the major problems are related to the immediate surface: (1) wall surface radiation damage; (2) plasma contamination. The former is due to beam irradiation decomposition and etching which results in a change in the surface structure and a possible reduction in the mechanical strength of the wall material. The latter is a result of releasing gaseous impurities from irradiated components which could lead to serious plasma

contamination. Niobium is one of the potential wall materials being considered for future CTR application. It would, therefore, be useful to study the radiation damage effect on niobium, particularly on "practical" specimens. The pentoxide is known to be formed on high purity niobium surface at relatively high oxygen pressure and moderate temperature [1, 2]. Therefore, the study of beam effects on Nb₂O₅ was included in this study. The effect of photon irradiation on oxidized niobium foil [3] and ion bombardment on Nb₂O₅ [4] have been reported. This paper presents a study of niobium oxide subjected to electron-beam irradiation using Auger electron spectroscopy (AES). It is known that a change of chemical environment can result in core level energy shifts and variation in valence-band density of states. This, in turn, can lead to different energies and shapes of Auger peaks. Therefore, from the change of Auger spectra under extended electron-bombardment, one is able to examine the beam effect on the specimen. The results obtained from electron stimulated desorption (ESD) study and a layer-by-layer calculation of contributions to the total Auger intensity from an altered overlayer are also presented to support the results observed in the AES study.

* Present address: 3M Co. Building 235-3F, 3M Center, St. Paul, Minnesota 55101, USA.

2. Experimental details

A Varian Auger system equipped with a cylindrical mirror analyser (CMA) with resolution better than 1% and Northern NS-570A digital signal analyser was used in this study. The measurements were carried out in an ambient pressure of 10^{-9} Torr and normal primary electron beam incidence was used in all measurements. Most measurements were done with beam energy at 3 keV, beam current density at 10 mA cm^{-2} , and modulation voltage at 3 V (peak-to-peak). The powder sample was prepared by pressing certified high purity (99.9%+, Ventron) Nb_2O_5 powder between indium foils (Material Research Corporation Martz grade). The niobium foil sample (Ventron m4N grade) was previously used in other experiments where the sample was repeatedly heated in 10^{-3} Torr of oxygen at less than 500 K. The exact composition of the oxide layer was not known. However, it was believed that the oxide layer consisted mainly of Nb_2O_5 with possibly small amounts of NbO_2 and NbO (at least for the outer several layers) as judged from the specimen preparation and its Auger spectrum. The foil specimen

was also found to be contaminated with S, Cl, C and N. The ESD measurements were done in a separate system with primary beam energy at 1 keV and incident beam current in the order of $\mu\text{A cm}^{-2}$. Only the foil specimen was used in the ESD measurement.

3. Results and discussion

3.1. Chemical shift

The most striking difference in the Auger MNN spectra of Nb_2O_5 and oxidized Nb foil from the corresponding standard spectrum of elemental niobium [5] was that the transition peaks involving valence electrons appear to be doublets. To be specific, they were $M_{4,5}N_1V$, $M_{4,5}N_{2,3}V$ and $M_{4,5}VV$ peaks (peaks f, g, and i in Fig. 1) and the separation of each doublet was 6, 4 and 6 eV respectively. Since the low-energy peak in each doublet existed only in the oxide state, one might name them as "oxide" peaks (f_1 , g_1 and i_1) to distinguish them from their doublet counterpart "metal" peaks (peaks f_2 , g_2 and i_2). "Metal" is used here to denote the peaks which grew as the reduction of the oxide proceeded, since the

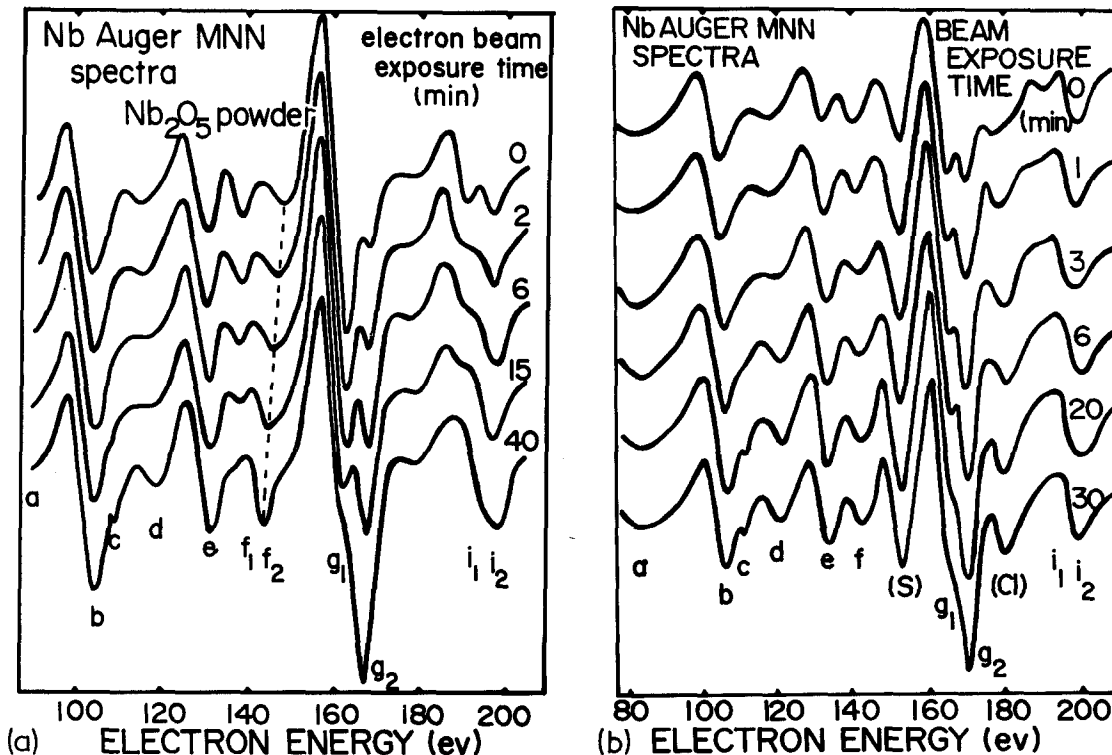


Figure 1 Variations of Nb Auger MNN spectra with beam exposure time. (a) Nb_2O_5 powder, beam voltage $E_p = 2 \text{ keV}$, beam current = $15 \mu\text{A}$, lock-in amplifier sensitivity $\text{SEN} = 0.1 \text{ mV}$, time constant $\text{TC} = 30 \text{ msec}$, modulation voltage $\text{MD} = 5 \text{ V}$ (peak to peak), sweep rate $\text{SR} = 4 \text{ V sec}^{-1}$. (b) oxidized Nb foil, the settings were the same as (a) except $\text{MD} = 3 \text{ V}$ and $\text{SR} = 5 \text{ V sec}^{-1}$.

reduction of the oxidation state usually caused the specimen to show more metal-like properties. The published X-ray photoelectron spectroscopy (XPS) measured values in the chemical shift due to oxidation ranged from 4.1 to 5.2 eV for the M_4 level and 5 to 5.7 eV for the M_5 level [6–10]. The chemical shift observed in AES was a resultant shift of the three levels involved in a particular transition. The chemical shift for each sublevel of the level N was not reported in the above published XPS measurements. It was, therefore, difficult to make a direct comparison of the published XPS results with the AES results obtained in this study. The chemical shift observed on other MNN-type transition peaks, namely $M_{4,5}N_1N_1$, $M_{4,5}N_1N_{2,3}$ and $M_{4,5}N_{2,3}N_{2,3}$ (peaks a, b and e) was less than 1 eV. This suggested that the relatively large chemical shift observed on the valence peaks was mainly due to the different density of states in the valence band between oxide and clean metal. It was possible to have “oxide” peaks in the oxide spectrum because of the cross-transition between niobium and oxygen in the oxide. The appearance of a doublet was a reflection of two distinct states in the valence band although other valence states might exist.

The binding energy difference between the O- $L_{2,3}$ level and Nb- $N_{4,5}$ level was about 4 eV [11]. It accounted for the chemical shift observed in the valence spectrum when one took into account the accuracy of using the relatively broad Auger peaks to determine the chemical shift. A larger shift was expected at the $M_{4,5}VV$ transition peak since the valence-band density of states was counted twice in determining the total Auger transition probability. For the $M_{4,5}N_1V$ transition, oxidation results in a splitting of the Nb 142 eV peak into a doublet pair at 140 and 146 eV in the Nb_2O_5 spectrum. A larger shift of the $M_{4,5}N_1V$ transition peak, ΔE_f , as compared to the shift of the $M_{4,5}N_{2,3}V$ transition peak, ΔE_g , was also expected. Since the bonding energy change due to oxidation of the N_1 level, ΔN_1 , is slightly smaller than the corresponding bonding energy change of the $N_{2,3}$ levels, therefore $\Delta E_f - \Delta E_g \approx \Delta N_{2,3} - \Delta N_1 > 0$. The existence of “metal” peaks in the initial Nb_2O_5 spectrum was probably due to the instant reduction of some surface Nb^{5+} upon electron beam exposure which would be discussed in the Section 3.2. In the case of oxidized Nb foil, the observation of $M_{4,5}N_1V$ was obscured by the presence of a large sulphur

impurity peak. The shifts for $M_{4,5}N_{2,3}V$ and $M_{4,5}VV$ peaks were the same as in Nb_2O_5 .

3.2. Beam irradiation effects

By exposing the specimen to the electron beam, the “metal” peak in each doublet grew at the expense of its “oxide” counterpart (Fig. 2). In the meantime, the Auger peak to peak height (APPH) of the oxygen KLL transition peaks reduces correspondingly, but no noticeable oxygen peak shifting was observed under beam exposure

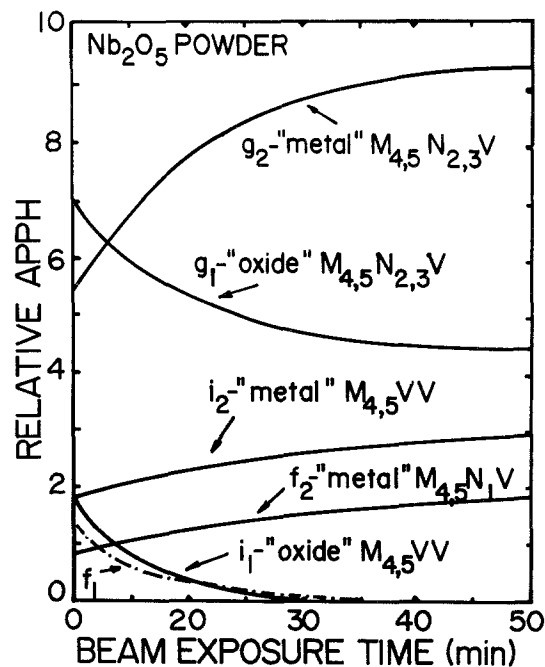


Figure 2 Changes in the three Nb_2O_5 valence doublet peaks with time of electron bombardment.

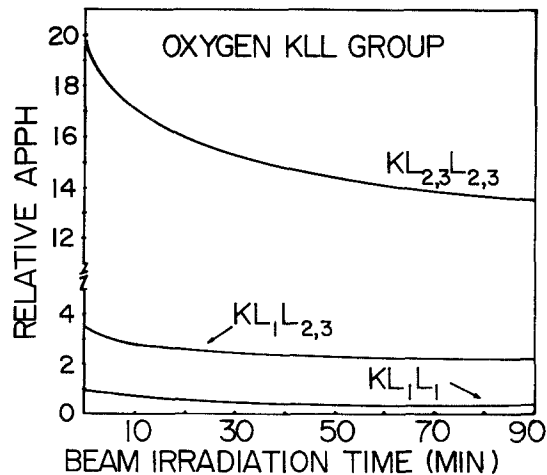


Figure 3 Oxygen KLL peak height variations in Nb_2O_5 with time of electron bombardment.

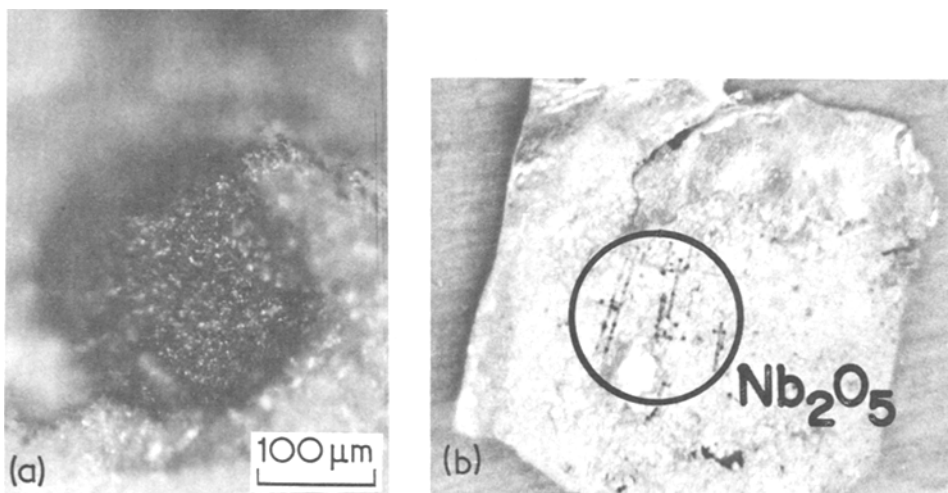


Figure 4 Colour change in the Nb_2O_5 powder surface with electron bombardment. (a) The circular dark area has been irradiated with 2 keV electrons of 1 mA cm^{-2} for 1 h. (b) Visible beam irradiation spots and beam tracks (within circle) produced after AES measurements.

(Fig. 3). The “metal” peak of $\text{M}_{4,5}\text{N}_{2,3}\text{V}$ and $\text{M}_{4,5}\text{VV}$ doublets stayed at a fixed position; while the “metal” peak of $\text{M}_{4,5}\text{N}_1\text{V}$ doublet shifted from 146 to 142 eV (the position of $\text{M}_{4,5}\text{N}_1\text{V}$ peak in the elemental Nb spectrum) during the electron irradiation process as indicated by a dotted line in Fig. 1a. The origin of this movement might have resulted from a significant peak shape change of the adjacent large $\text{M}_{4,5}\text{N}_{2,3}\text{V}$ peak and its plasmon loss peak during the oxide reduction process. The change of valence spectrum reflected a variation of valence band density of states. The near-metallic character of the surface of the electron-bombarded specimen could be determined from several features in the final Auger spectrum. (1) The position of niobium Auger peaks matched very well with the published standard spectrum of clean niobium [5]. (2) Several distinct plasmon energy loss peaks appeared at 110, 120 eV (peaks c, d, in Fig. 1) compared to the spectra of Nb_2O_5 and oxidized Nb foil. This was expected since the valence electrons in higher oxide states were more tightly bound than those in lower oxide and elemental metal states. Thus, they allowed fewer plasmon excitation losses. (3) A reduction of relative APPH ratio of oxygen to niobium. In order to obtain the correct relative concentration between oxygen and niobium, the APPH ratio must be multiplied by the relative elemental Auger sensitivity factor S between these two elements [5].

* $1 \text{ \AA} \equiv 10^{-4} \text{ \mu m}$.

$$\frac{C_{\text{O}}}{C_{\text{Nb}}} \approx \frac{\text{APPH}_{\text{O}}}{\text{APPH}_{\text{Nb}}} \cdot \frac{S_{\text{Nb}}}{S_{\text{O}}}$$

A more accurate method to estimate the relative concentration of each element will be discussed in Section 3.4. (4) Under the extended electron-bombardment, the variation of chemical environment for niobium atoms within its Auger escape depth ($\sim 7 \text{ \AA}$)* was greatly reduced. This resulted in an appearance of sharp Nb peaks in the final Auger spectrum. These observations clearly suggested an occurrence of beam induced dissociation and reduction of oxide effects. As a result, the specimen surface within the beam-exposed region was enriched with niobium. Murti and Kelly [3] have observed a reduction of Nb_2O_5 after bombarding the specimen with 35 keV Kr^+ . As a result, the sheet conductivity was found to increase by several orders of magnitude. The above-mentioned metal-like features in the final Auger spectrum seemed to indicate a similar conductivity enhancement could be observed on an electron-bombarded niobium oxide specimen.

The beam effects on niobium oxide was significant during the first 20 min of electron-bombardment with beam current density above 1 mA cm^{-2} . After that, the rate slowed down; and there was no significant variation of APPH ratio of Nb to O. Besides the exposure time, an important factor determining the beam effects was the incident-beam current density. The beam effects

dependence on the current density was observed in a range up to 200 mA cm^{-2} . The reduction rate dependence was nearly linear in the range below 130 mA cm^{-2} but increased dramatically after that. The effect was found to be less dependent on beam energy in the range of 1 to 3 keV.

No significant change in the carbon peak height was observed in the slightly carbon contaminated Nb_2O_5 powder specimen under extended electron bombardment. The carbon peak shape remained graphite-like in form indicating that no carbide build-up occurred under beam irradiation. Again, no carbide formation was observed on the foil specimen even though it showed a large amount of carbon contamination. However, it seemed that the existence of carbon impurity on oxidized foil specimen tended to reduce the oxide reduction rate as compared to the Nb_2O_5 powder specimen under the same dose of beam irradiation.

The beam irradiated region on the surface of both types of specimens could be easily recognized by a colour change (Fig. 4). This gave a further evidence of beam effect on the sample's surface composition as the white colour of Nb_2O_5 decreased and the dark colour of metallic and lower oxide (mostly NbO) mixture increased. The sensitivity of reduction of Nb_2O_5 upon electron-beam exposure was also indicated by the beam track left on the specimen almost instantly as one moved the beam from one point to another (Fig. 4b). Moreover, the specimens retained their

dark colours after several months of exposure to air at room temperature. This irreversible colour change seemed to indicate that the altered layer was more than 100 \AA thick.

3.3. ESD measurement

The AES observation of dissociation and reduction of surface oxide was further supported by ESD measurements. The ESD O^+ signal was found to increase steadily in the early stages of electron bombardment as shown in Fig. 5a. (Note that the beam current density used in ESD measurement was 3 to 5 orders of magnitude less than applied in AES analysis.) Fig. 5b shows that the O^+ signal dominates the ultimate ESD spectrum after several hours of electron bombardment. (A slight increase of H^+ and OH^+ signal was due mainly to the desorption of adsorbed H_2O and H_2 , since they were the main residual gases in the ESD measurement system.) The O^+ signal strength was an indirect indication of the surface concentration of oxygen species since the contribution to the O^+ signal from other species such as CO is small. The consecutive beam irradiation decomposition process $\text{Nb}_2\text{O}_5 \rightarrow \text{NbO}_x \rightarrow \text{NbO}$ or Nb lead to the creation of some weakly bound oxygen available for subsequent desorption. This accounted for the increase of the O^+ signal in the earlier stages of electron bombardment and its domination in the final ESD spectrum. The mechanism of these beam effects was primarily through a direct

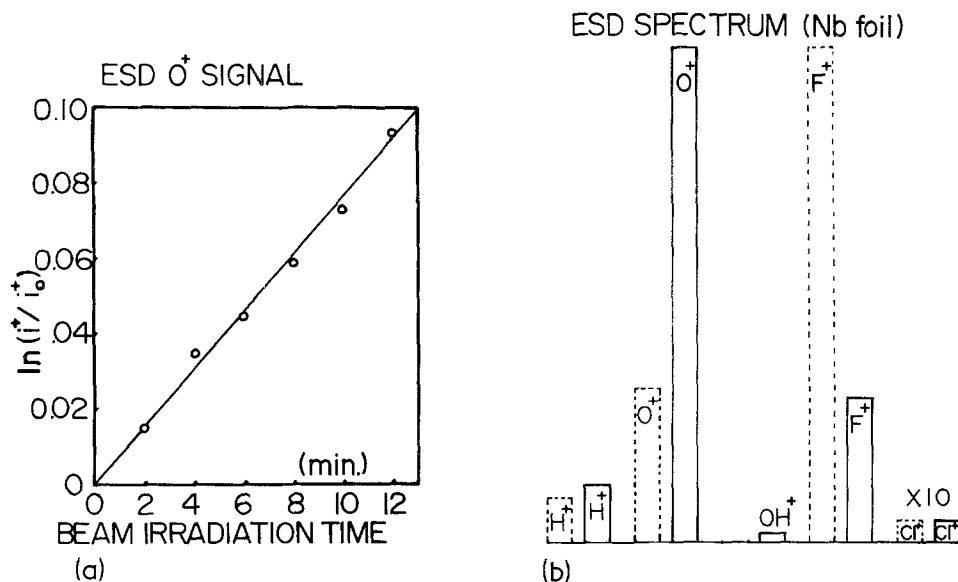


Figure 5 ESD measurement on oxidized Nb foil. Beam energy = 1 keV and beam current density = $4 \mu\text{A cm}^{-2}$. (a) Change of ESD O^+ signal with time of electron bombardment. (b) ESD spectra, dotted line, initial state, solid line, after 5 h electron-bombardment.

incident beam excitation with a small percentage possibly through indirect thermal excitation.

3.4. Calculation of Auger intensity

Each atomic plane's contribution to the total Auger intensity can be calculated by a layer-by-layer model proposed by Dobson and Regan [12]. The total measured Auger intensity due to the emission of a XYZ transition Auger electron from element i can be approximated as:

$$I_i(E) \Big|_{xyz} = K_{n,i}(E) \Big|_{xyz} \times \sum_{n=1}^{10} A_{n,i} \exp \left[-\frac{(n-0.5)}{\lambda_i \cos \theta} d \right] \quad (1)$$

(for a CMA analyser and $\theta = 42.5^\circ$)

where

$$K_{n,i}(E) \Big|_{xyz} = \frac{1}{2} j_n(E) \sigma_{i,x}(E) P_{n,i} \Big|_{xyz} \sin \theta$$

$j_n(E)$ = the incident beam flux (of energy E) at the n th layer,

$\sigma_{i,x}(E)$ = the ionization cross-section for the core level x in element i by electrons with energy E ,

$P_{n,i} \Big|_{xyz}$ = the probability that an excited element i on the n th layer will emit an xyz transition Auger electron,

$A_{n,i}$ = the layer density of the element i on the n th layer,

$n - 0.5$ = the correction factor used to account for the absorption by emitting atomic layer n ,

d = the interlayer spacing,

λ_i = the mean free path for an Auger electron from element i ,

$\exp \left[-\frac{(n-0.5)}{\lambda_i \cos \theta} d \right]$ = the escape probability for an Auger electron originating from the n th layer and directed along a path making an angle θ to the surface normal,

and $K_{1,i}(E) \simeq K_{2,i}(E) \simeq \dots K_{10,i}(E)$.

By comparing the measured APPH ratio of oxygen to niobium with that calculated for different overlayer structures, the possible overlayer structure of a specimen can be obtained.

$$\frac{I_O/I_{Nb}}{I'_O/I'_{Nb}} = \frac{\text{APPH}_O/\text{APPH}_{Nb}}{\text{APPH}'_O/\text{APPH}'_{Nb}} \quad (2)$$

where prime denotes the corresponding values in the altered state.

For simplicity, one can assume that an atomically flat specimen has a uniform layer density of Nb and O and constant interlayer spacing (3 Å) throughout the overlayer of Nb₂O₅. The mean free paths for Nb (168 eV) and O (512 eV) Auger electrons were assumed to be 7 and 10 Å respectively. The colour change indicated that the electron beam irradiation effects the surface composition into deeper layers than the AES probe range (less 20 Å). For the purpose of Auger intensity calculation, we can still confine the calculation to the outer 10 layers. Again for simplicity, uniform layer density of Nb and O and constant interlayer spacing for the altered overlayer was assumed. The calculated result showed that the altered overlayer which consisted of 50% niobium was formed on the powder specimen upon extended electron bombardment. In the oxidized niobium foil case, the exact composition of oxide layer is not certain; therefore, two different compositions were assumed in the calculation. One was Nb₂O₅ and the other was assumed to be 60% Nb₂O₅, 20% NbO₂ with 20% NbO. The results showed that the altered layer of an oxidized Nb foil specimen for the above two different compositions was found to be enriched with 40 and 53% of Nb, respectively, due to beam irradiation. Therefore, the calculated results indicated a reduction of oxide in both cases. The degree of composition alteration was not expected to be uniform throughout the altered overlayer. The change was greater for the outermost several layers where direct beam irradiation induced decomposition and preferential removal of oxygen played an important role. The change in deeper layers was probably due mainly to irradiation-enhanced diffusion. Therefore, the actual concentration percentage for niobium may be higher in the outermost several layers.

The observations outlined above clearly showed that the electron beam can greatly alter the composition of niobium oxide under particular conditions. Therefore, some precaution must be taken when studying niobium oxide compounds using a combination of AES and simultaneous ion-beam sputter etching technique, since the sputter-etch rate can increase within the electron-beam illuminated area. The enhancement of the sputter-etch rate could clearly be of concern in the CTR project if niobium is adopted as first wall material. In

addition, the process would effect plasma contamination due to the preferential removal of oxygen under continuous charged particle impact.

4. Conclusions

The Auger spectra of both oxidized Nb foil and Nb₂O₅ specimens showed a peak splitting feature with a MNN-type Auger transition involving valence electrons, as compared to the corresponding spectrum of clean niobium. The doublet valence peaks were a reflection of contribution of Nb-4d and O-2p states in the valence band of niobium oxide. The spectrum of an extended electron-bombarded specimen showed a reduction of both surface Nb⁵⁺ and oxygen concentration. In addition, the beam irradiation induced decomposition of oxide and loss of oxygen were further supported by the colour change in the beam irradiated region, ESD measurements and a layer-by-layer calculation of the contribution to total Auger intensity from each atomic plane of an altered overlayer.

Acknowledgements

This work is supported by ERDA grant no. EY-76-S-02-2425 and NSF grant no. DMR-74-03947. It is a pleasure to acknowledge the valuable discussions with Dr G. Burland. The ESD data supplied by Dr M. Drinkwine is also acknowledged.

References

1. R. F. VOITOVICH, in "Surface Interactions Between Metals and Gases", V. I. Arkharov and K. M. Gorbunova (eds.) (Consultants Bureau, NY, 1966), p. 132.
2. H. H. FARRELL, H. S. ISAACS and M. STRONGIN, *Surf. Sci.* **38** (1973) 31.
3. D. LICHTMAN and T. T. LIN, Proceedings of 7th International Vacuum Congress and 3rd International Conference on Solid Surfaces in Vienna, Austria, 12-16 September (1977).
4. D. K. MURTI and R. KELLY, *Surf. Sci.* **47** (1975) 282; *Idem. Thin Solid Films* **33** (1976) 149.
5. L. E. DAVIS, N. C. MacDONALD, P. W. PALMBERG, G. E. RIACH and R. E. WEBER, "Handbook of Auger Electron Spectroscopy" (Physical Electronics Industries, Inc., Eden Prairie, MN 1976) 2nd edn, p. 127.
6. T. NOVAKOV and T. H. GEBALLE, *Solid State Commun.* **10** (1972) 225.
7. M. K. BAHL, *J. Phys. F-Metal Phys.* **4** (1974) 497.
8. R. CAILLAT, R. FONTAINE, L. FEVE and M. J. GUITTET, *Compt. Rend Acad. Sci. (French), Ser. C* **280** (1975) 189.
9. *Idem, ibid* **283** (1976) 273.
10. D. SIMON, C. PERRIN and P. BAILLIF, *ibid Ser. C* **283** (1976) 241.
11. J. A. BEARDEN and A. F. BURR, *Rev. Mod. Phys.* **39** (1967) 125.
12. P. J. DOBSON and B. J. REGAN, *J. Phys. E* **9** (1976) 694.

Received 8 May and accepted 10 July 1978.